Redox Catalysis Using $Ag@SiO_2$ Colloids

Thearith Ung,[†] Luis M. Liz-Marzán,*[,‡] and Paul Mulvaney*[,†]

Nanotechnology Laboratory, School of Chemistry, University of Melbourne, Parkville, 3052, Australia, and Departamento de Química Física, Facultade de Ciencias, Universidade de Vigo, 36200, Vigo, Spain

Received: April 1, 1999

We show that metal particles encapsulated by thin silica shells can catalyze redox reactions on their surface. The surface charge of both silica-coated and uncoated colloidal silver particles has been varied by chemical electron injection, using controlled amounts of borohydride ions. The charging and discharging processes were monitored by time-resolved UV−visible spectroscopy, making use of the influence of the surface charge on the position and intensity of the silver plasmon band. We show that the charging and discharging rates can be controlled by means of silica coating, since they are limited by the diffusion of borohydride ions through the silica pores.

Introduction

There has been intense study of the process of redox catalysis on small metal particles because of its importance to most commercial hydrogenation reactions[1,2] and to practical, photolytic water-splitting schemes.[3] Catalytic particles are normally generated by direct reduction of metal salts that have been allowed to diffuse into support materials such as silica,[4] zeolites,[5] and alumina.[6] There is little control over the shape or morphology of such particles, and their dispersion within the support is usually difficult to specify.

The reason for the direct reduction of small salts rather than adsorption into the support after preparation is first to minimize the amount of coalescence of the primary nuclei, which are normally the most active catalysts. Second, formation in a bulk solvent necessitates the presence of particle stabilizers[7−9] to prevent coalescence and particle growth. In some cases, it has been shown that these stabilizers themselves undergo chemical reactions on the surfaces they protect. For example, Kopple et al. showed that poly(vinylsulfonate) suffered H abstraction on the surface of colloidal Pt under reducing conditions.[10,11] Furthermore, the actual surface coverage of adsorbed stabilizers is usually unknown, and in some cases, they may even retard catalysis by blocking active sites. Consequently, it would seem advantageous to create catalyst particles with a well-defined, variable, and permeable coating for uses in general redox catalysis.

It was recently reported[12−14] that noble metal particles such as Ag and Au could be coated with thin silica shells of well-defined thickness. While these shells have obvious importance as colloid stabilizers, such dense layers would appear to render the core catalytically inert and to be of little practical utility. In this work, we therefore investigated the possible use of metal−silica core−shell particles as model catalysts and we examined whether the silica shell can act as a selective membrane for catalysis.

To monitor the processes of electron injection and discharge, we use the fact that the surface plasmon band of colloidal silver undergoes a blue shift when the electron density is increased, and red-shifts during electron transfer to solution oxidants.[15,16] The aim in this initial report is to demonstrate that redox catalysis is possible with $Ag@SiO_2$ particles and that control of the rate of catalysis is possible by tuning the silica shell thickness.

Experimental Section

1. Materials. (3-Aminopropyl)trimethoxysilane or APS from Aldrich, sodium silicate solution ($Na_2O(SiO_2)_{3-5}$, 27 wt % SiO_2) (Aldrich), $AgClO_4 \cdot H_2O$ (Sigma), $NaBH_4$ (Aldrich), trisodium citrate dihydrate (Aldrich), and poly(acrylic acid) (MW 2000, Sigma) were used as received. Analytical grade ethanol and Milli-Q grade water were used in all the preparations. All other chemicals were analytical grade and used as supplied by the vendor. Transmission electron microscopy (TEM) was carried out with a Philips CM10 microscope; particle sizes and silica shell thicknesses were measured from several negatives of each sample. UV−visible spectra were measured with a Hewlett-Packard Diode Array HP8453 spectrophotometer.

2. Colloids Preparation. PAA-protected silver colloids were prepared by rapidly adding a mixture of 1 mL 0.01 M $AgClO_4$ and 0.5 mL 0.02 M PAA (MW 2000) to 98.5 mL of vigorously stirred, ice cold water containing 1 mM $NaBH_4$. The solution turned bright yellow immediately. The particles so prepared had a mean diameter of 10 nm.

Citrate-protected silver was prepared by rapidly adding 1 mL of 0.01 M $AgClO_4$ to 99 mL of a vigorously stirred, ice-cold solution containing 1 mM $NaBH_4$ and 0.30 mM sodium citrate. The final colloid was also bright yellow, and the mean particle size was also close to 10 nm.

The preparation of $Ag@SiO_2$ colloids involves three basic steps. First, the surface of citrate−silver is activated with APS to generate siloxy groups receptive to silicate ion deposition. Then, addition of sodium silicate ion at supersaturated concentrations leads to an initial nanometer thick mantle, and finally controlled precipitation of residual silicate by addition of ethanol creates a homogeneous shell (see Figure 1). Details on the deposition of silica shells with various thicknesses can be found in ref 14.

Charging and discharging processes were monitored as follows. Typically, 0.2 mL of ice-cold 6 mM $NaBH_4$ was added

* Corresponding authors. E-mail: p.mulvaney@chemistry.unimelb.edu.au. Fax: + 61 3 9344 6233. E-mail: lmarzan@uvigo.es. Fax: + 34 986812382.
[†] University of Melbourne.
[‡] Universidade de Vigo.

10.1021/jp991111r CCC: $18.00
Published on Web 08/12/1999

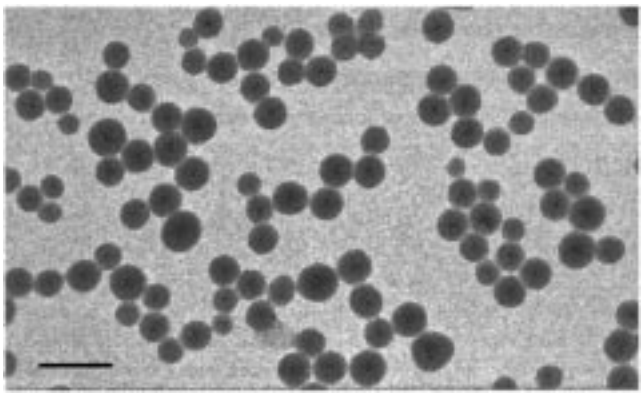

Figure 1. Transmission electron micrograph of $Ag@SiO_2$ particles with average core diameter of 10 nm and shell thickness 15 nm. Scale bar is 100 nm.

rapidly to 2 mL of 0.1 mM uncoated or coated silver sol with magnetic stirring. Once the borohydride solution was injected, spectral measurement was triggered and the absorption spectrum was recorded continuously using the diode array spectrophotometer. When varying the $NaBH_4$ concentration, the same volume was added to keep the silver sol concentration constant for all experiments.

Theory

It is well-known that small metal particles display strong absorption bands in the UV−visible part of the spectrum due to resonant absorption of light by the conduction electrons. For silver, the position of the resonance band is accurately given by[17]

$$\lambda_{peak}{}^2 = \lambda_P{}^2(\epsilon^\infty + 2\epsilon_m) \quad (1)$$

where $\lambda_P{}^2 = 4\pi^2c^2m\epsilon_o/Ne^2$ is the bulk plasma wavelength in terms of the electron mass, vacuum permittivity ϵ_o, the electron charge e, and the electron density N; ϵ^∞ is the high-frequency dielectric constant of silver (about 4.9 ± 0.3[16]), and ϵ_m is numerically equal to the square of the solvent refractive index, which for water is 1.78.

Changes in the excess electron charge due to double layer charging alter the value of N. For small particles, a change of 100 mV typically alters the surface charge density by about 1%, which is readily monitored spectroscopically[15] and in fact is discernible to the naked eye. For coated particles, there is a correction needed for the effect of the shell layer. This shell simply causes a shift of the absorption band to longer wavelengths by 5−6 nm,[13,14] and this is not important except for absolute peak determination.

Results and Discussion

1. Charging of PAA- and Citrate-Stabilized Silver Colloids. To study charge injection, we use the oxidation of borohydride. Upon addition to the sol, the particles are cathodically polarized by the reaction[19]

$$BH_4{}^- + Ag_n + 3H_2O \rightarrow BO_3{}^{3-} + Ag_n{}^{8-} + 10H^+ \quad (2)$$

This reaction is probably diffusion limited given the large negative redox potential for BH_4^- oxidation ($E_o = -1.2$ V). Though the injection of electrons occurs within a minute or two, the subsequent discharge processes are much slower. This is due to the high overpotential for hydrogen evolution on silver

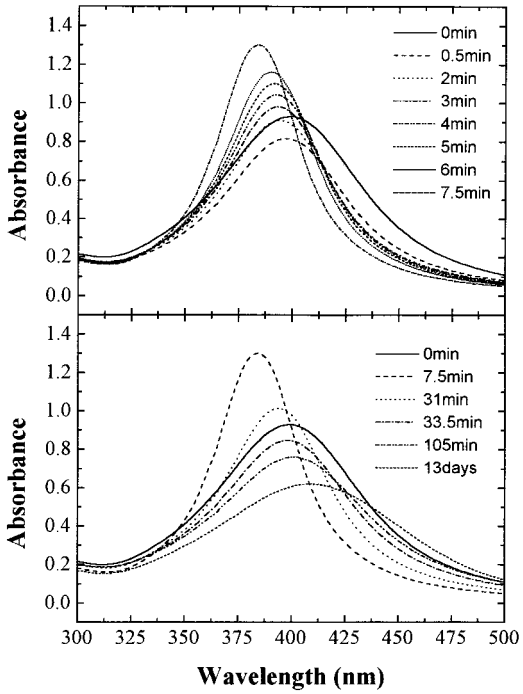

Figure 2. Time evolution of the absorption spectra of the PAA-stabilized silver upon addition of 0.55 M $NaBH_4$: upper, charging period; lower, discharging period.

metal. Since any dissolved oxygen is immediately consumed by BH_4^- upon addition to the sol and the pH rises quickly to about 10.3 due to direct reaction of borohydride with water molecules, the major discharge reaction is

$$8H_2O + Ag_n{}^{8-} \rightarrow Ag_n + 4H_2 + 8OH^- \quad (3)$$

From eq 1, we see that the charge density on the particle surface influences the plasmon absorption of metallic colloids. In ref 15, it was shown that a change in surface potential of PAA-protected silver from 0.0 V to −0.40 V vs Ag/AgCl induced a blue shift of some 10 nm, as well as a decrease in absorbance and broadening of the plasmon band, in accordance with theory.

In the experiments that we are presenting here, the injection of borohydride ions into a silver sol with no free Ag^+ ions present will likewise increase the overall negative charge on the particle. In fact, we have observed for both PAA−silver and citrate−silver (Figures 2 and 3, respectively) that upon borohydride injection a blue shift, band sharpening, and an increase in the band intensity all take place simultaneously. Actually, the first effect is a small but rapid decrease in intensity, which is more important for citrate−silver. This is probably due to the adsorption of borohydride ions onto the surface, with no immediate charge transfer. Following the blue shift, the reverse process is observed, i.e., there is a red shift, band broadening, and a decrease of maximum intensity. This undoubtedly points toward a discharging process. Charging persists until the maximum charge density on the particle surface is achieved, then the charge remains constant until the borohydride concentration is insufficient to maintain the electron density on the particles so that spontaneous "oxidation" of the surface occurs, probably via reduction of water or other moieties resulting from borohydride oxidation.

Analysis of Figures 2−4 shows that, although the qualitative effect is the same for both types of sols, there are some quantitative differences. First, the charging rate (as deduced from

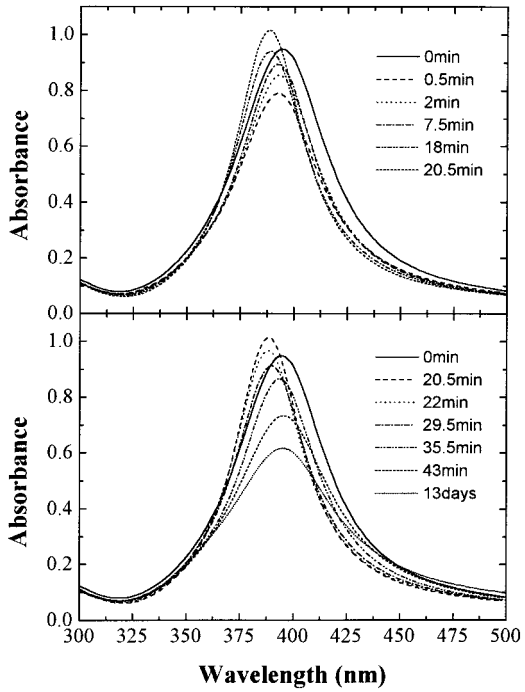

Figure 3. Time evolution of the absorption spectra of the citrate-stabilized silver upon addition of 0.55 M $NaBH_4$: upper, charging period; lower, discharging period.

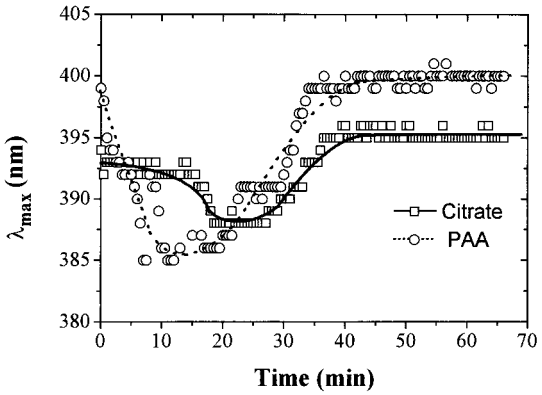

Figure 4. Time evolution of the maximum position for citrate and PAA-stabilized silver sols upon addition of 0.55 M $NaBH_4$.

the time required to achieve the minimum value of λ_{max}) is faster for PAA−silver. With respect to the discharging process, one can see in Figure 4 that the time taken for the discharge to occur and the peak to move to longer wavelengths is virtually identical for both samples. We also note that the size of the spectral shift (maximum peak position − minimum peak position) is significantly larger for PAA−Ag colloids, indicating that there is a larger steady state electron density during cathodic polarization. The fact that the spectrum is more strongly red shifted after discharge is probably due to adsorption of borate ions on the silver particles once borohydride has been completely oxidized. This was confirmed through the following experiment. Fresh $NaBH_4$ was boiled for 30 min to completely oxidize all BH_4^- to BO_3^{3-} or other decomposition products. This solution was left to stand for a further 24 h. It was added at the same concentrations as $NaBH_4$ for the charging experiments to a PAA−Ag colloid. The surface plasmon band was decreased in intensity immediately by about 10−15% (from 0.79 to 0.69) and slightly red shifted from 399 to 403 nm. From this, it seems the decomposition products from the borohydride do adsorb and cause red shift and some damping of the band.

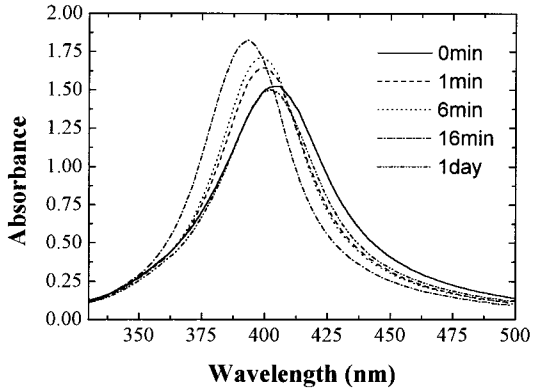

Figure 5. Time evolution of the absorption spectra of $Ag@SiO_2$ (shell thickness = 15 nm) upon addition of 0.55 M $NaBH_4$.

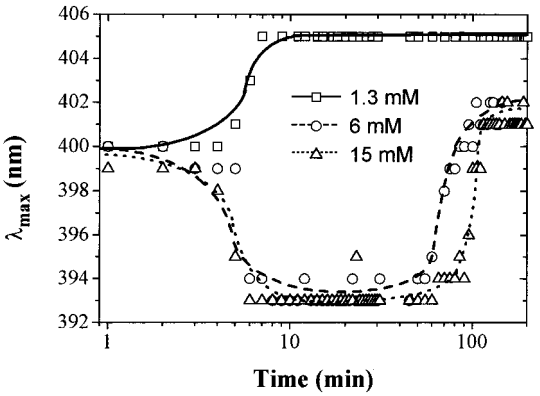

Figure 6. Time evolution of the maximum position for $Ag@SiO_2$ (shell thickness = 15 nm) upon addition of $NaBH_4$ with various concentrations. Time log scale was chosen for better clarity.

2. Charging of $Ag@SiO_2$ Colloids. It has been shown that the deposition of (thin) silica shells onto metal[12−14] and semiconductor[20] nanoparticles leads to enhanced stability in aqueous dispersion so that aggregation is prevented, even after successive modification of the silver surface, which is not in direct contact with the solvent. A second favorable feature of $Ag@SiO_2$ for the present experiment is the porous nature of the silica shell, which permits reactant diffusion from solution inward and back to solution.[14,21] Therefore, in this case, there must be an additional contribution to the control of the charging process: diffusion of reactants and products through the porous silica shell. In ref 14, it was shown that the uniformity of the silica shells deposited onto silver nuclei increases with thickness, which motivated the use of relatively thick shells in this work (Figure 1). An example of the time evolution for $Ag@SiO_2$ with 15 nm thick shells, under the same conditions as for Figures 2 and 3, is shown in Figure 5. Although there is again qualitative coincidence with the results for PAA−silver and citrate−silver, some noticeable differences can be observed. First of all, there is no initial damping of the plasmon band, which means that the surface is not altered apart from charge injection. The time required for reaching the minimum λ_{max} value is comparable to that for the previous systems, showing a rather rapid diffusion of borohydride through the shell. Additionally, the final spectrum is very similar to the initial one, with just a slight sharpening and blue shift of the plasmon band.

In Figure 6, the time evolution of λ_{max} for experiments on the same system but with varying borohydride concentrations are shown. From this figure, several features of the process can be extracted. When a low borohydride concentration is used, there is insufficient electron injection to affect the particles. The

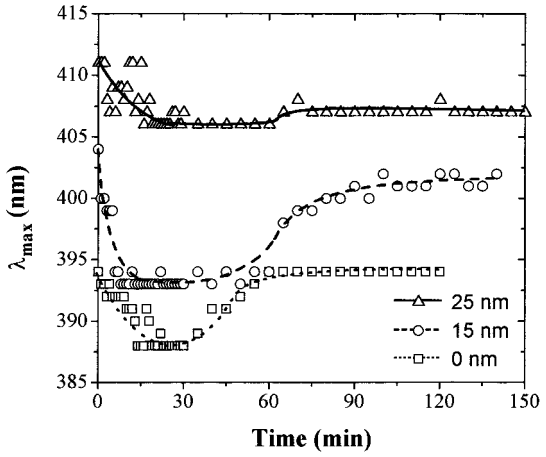

Figure 7. Influence of silica shell thickness on the time evolution of the maximum position for $Ag@SiO_2$ upon addition of 0.55 M $NaBH_4$.

only effect observed is a quick blue shift followed by immediate recovery of the band to its initial value. For an intermediate concentration (5 times larger than before), the initial blue shift is larger, and a red shift back to (close to) the original value of λ_{max} is not achieved until some 2 h after injection. For even larger borohydride concentrations, the wavelength shift is the same as before, and the only difference is that the particles remain polarized, i.e., the band remains at the minimum λ_{max} longer. It is remarkable that the final band position is independent of the borohydride concentration used.

Finally, we studied the influence of the thickness of the silica shell on the time evolution of λ_{max} (see Figure 7). One can see in the figure that, the thicker the silica shell, the longer it takes to reach the maximum blue shift, which agrees well with the reactant diffusion model proposed in ref 14. Additionally, it is also observed that for thicker shells the final position of the plasmon band is more blue shifted, which seems to be linked to the capacity of the shells to store adsorbed borohydride ions.

The spectroscopic data clearly prove that the metal core particles remain catalytically active despite the presence of the silane coupling agent and the silica shell. The rate of spectral shift is not noticeably reduced by thin silica shells, so small redox molecules can clearly diffuse through rapidly. We have no information on the local pH at the silver core, though it could be up to 2 pH units lower than in the bulk solution, due to ionization of pore surface silanols.

Importantly, the particles do not show shell decomposition due to gas pressure from the hydrogen evolution reaction, which suggests that hydrogen gas diffuses back out into bulk solution. It has been shown previously[21] that the build up of solid products inside nanometer thick silica shells can cause shell rupture.

Conclusions

While we have not demonstrated that the silver particles within silica shells are any more catalytically active than conventional sols, we have shown the feasibility of using them as stable nanoreactors for redox catalysis and confirmed that they will not undergo particle coalescence during catalysis. Furthermore, based on the slower rates of borohydride oxidation found for thicker shell layers, we expect that the shell can act as a size-selective membrane, which can be used to alter the chemical yields for competing catalytic reactions. This core−shell catalysis geometry also opens up the possibility of more rigorous study of mixed catalysts. These can be prepared and characterized in bulk solution before encapsulation, allowing systematic variation of metal composition, alloying, and shell structure to be investigated.

Acknowledgment. T.U. is grateful for receipt of an Australian Postgraduate Award. This work was supported by a grant from the Australian Research Council and by the Spanish Xunta de Galicia (Project XUGA30105A97). L. M. Liz-Marzán acknowledges support from NATO Collaborative Research Grant CRG 971167.

References and Notes

(1) Foger, K. In *Catalysis Science and Technology*; Anderson, J. R., Bouchart, M., Eds.; Springer-Verlag: Berlin, 1984; Vol. 6, pp 227−307.

(2) Bradley, J. S. In *Clusters and Colloids. From Theory to Applications*; Schmid, G., Ed.; VCH: Weinheim, 1994.

(3) Kiwi, J.; Grätzel, M. *J. Am. Chem. Soc.* **1979**, *101*, 7214.

(4) Sinfelt, J. H.; Via, G. H. *J. Catal.* **1979**, *56*, 1.

(5) Manninger, I.; Paál, Z.; Tesche, B.; Klengler, U.; Halász, J.; Kiricsi, I. *J. Mol. Catal.* **1991**, 361.

(6) Tan, B. J.; Klabunde, K. J.; Sherwood, M. A. *J. Am. Chem. Soc.* **1991**, *113*, 855.

(7) Rampino, L. D.; Nord, F. F. *J. Am. Chem. Soc.* **1942**, *63*, 2745.

(8) Furlong, D. N.; Launikonis, A.; Sasse, H. F.; Sanders, J. V. *J. Chem. Soc., Faraday Trans. 1* **1984**, *80*, 571.

(9) Esumi, K.; Itakara, T.; Torigoe, K. *Colloid Surf. A* **1994**, *82*, 111.

(10) Kopple, K.; Meyerstein, D.; Meisel, D. *J. Phys. Chem.* **1980**, *84*, 870.

(11) Meisel, D.; Mulac, W. A.; Matheson, M. S. *J. Phys. Chem.* **1981**, *85*, 179.

(12) Liz-Marzán, L. M.; Giersig, M.; Mulvaney, P. *Chem. Commun.* **1996**, 732.

(13) Liz-Marzán, L. M.; Giersig, M.; Mulvaney, P. *Langmuir* **1996**, *12*, 4329.

(14) Ung, T.; Liz-Marzán, L. M.; Mulvaney, P. *Langmuir* **1998**, *14*, 3740.

(15) Ung, T.; Dunstan, D.; Giersig, M.; Mulvaney, P. *Langmuir* **1997**, *13*, 1773.

(16) Rostalski, J.; Quinten, M. *Colloid Polym. Sci.* **1996**, *274*, 648.

(17) Mulvaney, P. *Langmuir* **1996**, *12*, 788.

(18) Kreibig, U. *J. Phys. F: Met. Phys.* **1974**, *4*, 999. Kreibig, U. *J. Phys. (Paris)* **1977**, *38*, C2-97.

(19) Schlesinger, H. I.; Brown, H. C.; Finholt, A. E.; Gilbreath, J. R.; Hoekstra, H. R.; Hyde, E. K. *J. Am. Chem. Soc.* **1953**, *75*, 215.

(20) Correa-Duarte, M.; Giersig, M.; Liz-Marzán, L. *Chem. Phys. Lett.* **1998**, *286*, 497.

(21) Giersig, M.; Ung, T.; Liz-Marzán, L. M.; Mulvaney, P. *Adv. Mater.* **1997**, *9*, 570.